

MODELLING OF NECTARINE DRYING UNDER NEAR INFRARED – VACUUM CONDITIONS

Behnam Alaei, Reza Amiri Chayjan✉

Department of Biosystems Engineering, Faculty of Agriculture, Bu-Ali Sina University, Hamedan, Iran

ABSTRACT

Background. Drying of nectarine slices was performed to determine the thermal and physical properties in order to reduce product deterioration due to chemical reactions, facilitate storage and lower transportation costs. Because nectarine slices are sensitive to heat with long drying period, the selection of a suitable drying approach is a challenging task. Infrared-vacuum drying can be used as an appropriate method for susceptible materials with high moisture content such as nectarine slices.

Material and methods. Modelling of nectarine slices drying was carried out in a thin layer near infrared-vacuum conditions. Drying of the samples was implemented at the absolute pressures of 20, 40 and 60 kPa and drying temperatures of 50, 60 and 70°C. Drying behaviour of nectarine slices, as well as the effect of drying conditions on moisture loss trend, drying rate, effective diffusion coefficient, activation energy, shrinkage, colour and energy consumption of nectarine slices, dried in near infrared-vacuum dryer are discussed in this study. Six mathematical models were used to predict the moisture ratio of the samples in thin layer drying.

Results. The Midilli model had supremacy in prediction of nectarine slices drying behaviour. The maximum drying rates of the samples were between 0.014–0.047 $\frac{g_{\text{water}}}{g_{\text{dry material}}}$ ·min. Effective moisture diffusivity of the samples was estimated in the ranges of $2.46 \cdot 10^{-10}$ to $6.48 \cdot 10^{-10}$ m²/s. Activation energy were computed between 31.28 and 35.23 kJ/mol. Minimum shrinkage (48.4%) and total colour difference (15.1) were achieved at temperature of 50°C and absolute pressure of 20 kPa. Energy consumption of the tests was estimated in the ranges of 0.129 to 0.247 kWh.

Conclusion. Effective moisture diffusivity was increased with decrease of vacuum pressure and increase of drying temperature but effect of drying temperature on effective moisture diffusivity of nectarine slices was more than vacuum pressure. Activation energy was decreased with decrease in absolute pressure. Total colour difference and shrinkage of nectarine slices on near infrared-vacuum drying was decreased with decrease of vacuum pressure and decrease of drying temperature.

Key words: nectarine, vacuum dryer, moisture diffusivity, activation energy, shrinkage

INTRODUCTION

Nectarine (*Prunus persica*) is smooth-skinned peach of the rosaceae family, known for more than 2000 years and grown throughout the warmer temperate regions of both the northern and southern hemispheres. In tree shape and leaf characteristics the peach and nectarine are indistinguishable, but nectarine fruits

look more like plums than peaches because of the smooth skin. The stones and kernels of the two fruits are alike in appearance. Nectarines have red, yellow or white flesh and source of fiber, iron, calcium, magnesium, phosphorus, zinc, copper, glucose and vitamin B₁, B₂, B₃, B₆, C and E (Balch, 2003). Nectarine is one of

✉ amirireza@basu.ac.ir, phone +98 811 442 4014, fax +98 811 442 4012

the most commonly consumed fruits in several countries. However, ripened nectarine is perishable and deteriorates rapidly after harvesting, hence the need to apply an appropriate postharvest technology to prolong the shelf life of the fruit and drying is among the most popular methods for the purpose. Therefore, drying and preservation are very important for household consumption, as well as for commercial additives.

Drying is one of the oldest and most important thermal processing techniques aimed at reducing water activity, inactivate enzymes and restrain deteriorative microbial growth (Avila and Silva, 1999; Maskan, 2000; Krokida et al., 2001). However, traditional drying techniques impart an adverse effect on quality and organoleptic properties of foods mainly because of physicochemical changes occurring in the tissue during drying. Hence kinetic models of thermal degradation are essential to design new processes to get a safe food product and giving a maximum retention of quality factors (Barreiro et al., 1997; Ibarz et al., 1999; Dadali et al., 2007a, 2007b).

Wavelength of some electromagnetic waves is as follows: ultraviolet waves (UV) including short length waves from 290 to 320 nm (UVB) and long length waves from 320 to 400 nm (UVA) (Harold, 2008). The visible wavelength (VIS) range is from 400 to 800 nm. Infrared waves (IR) is included near infrared (NIR) with short length waves from 700 to 2500 nm and mid infrared (MIR) with medium length waves from 2500 to 10 000 nm and far infrared (FIR) with long length waves from 10 to 1000 μm (Reich, 2005).

Major part of near-infrared radiation energy impinges upon a grain surface and penetrates about 1 mm under the surface into the grain (Ginzburg, 1969; Nindo et al., 1995). All of near-infrared radiation energy is completely absorbed by the surface grain molecules (Sandu, 1986). This phenomenon leads to the rapid heating of moisture inside the grain (Sakai and Hanzawa, 1994; Ratti and Mujumdar, 1995; Meeso et al., 2007). After heating of grain, moisture transfer from the interior layers occurs. This mechanism is similar to microwave heating process (Sakai and Hanzawa, 1994). As a result reduction of moisture gradient occurs, as well as the stresses development within a product, hence the product quality is maintained (Meeso et al., 2004).

Infrared radiation drying is appropriate especially for thin layer and slices of products. In this method,

heating the product is performed without undesirable changes in structure, so the structural quality of the product is improved, its biological yield is increased and costs of operation are decreased (Strumillo and Kudra, 1987). Another advantage of drying using infrared radiation is minimization of product losses such as colour change and shrinkage. Also IR radiation causes rapid and direct heat concentration on the material compared to the convective dryers in which part of the heat is absorbed by the inlet air and wasted. IR drying method in fact developed for high drying rate without the risk of burning the material (Nonhebel, 1973). Infrared radiation has been used in conjunction with several drying methods because it has advantages of increasing the drying efficiency (Ratti and Mujumdar, 1995).

To counter the undesirable effects of IR drying method and to improve the product quality, as well as nutritional value a potentially useful technique called vacuum drying is recommended. It allows effective moisture elimination under low pressure (Jaya and Das, 2003). Vacuum drying enhances the mass transfer because of an increased vapour pressure gradient between the inside and outside of the product (Pere and Rodier, 2002).

Combination of near infrared and vacuum can provide a fast and quality method for thin layer drying. The main goals of this study were to determine the effect of drying temperature and vacuum pressure on nectarine slices in near infrared-vacuum dryer, to evaluate a suitable drying model for describing the drying process and to compute drying rate, model effective moisture diffusivity, activation energy, shrinkage, colour and energy consumption of the drying samples.

MATERIAL AND METHODS

Sample preparation. Fresh nectarine samples were procured from a local market. After thorough cleaning and washing, the nectarines were cut into 2.8 mm thickness then the fruit was cut to cylindrical shape by a ring cutter with inner diameter of 28 mm. Weight of each sample was about 45 ± 2 g and a single layer was placed on the tray dryer. All experiments were performed in triplicates. Drying of the samples was implemented at the air temperatures of 50, 60 and 70°C and absolute pressures of 20, 40 and 60 kPa.

Air relative humidity and ambient air temperature during drying changed from 23 to 34% and 23 to 31°C, respectively. Initial moisture content of nectarine was determined using gravimetric method at 70°C for 24 h (AOAC, 2002). Initial moisture content of nectarine was 5.52% (d.b.). Final moisture content of nectarine slices after drying process was about 0.09% (d.b.).

Experimental setup. A schematic view of the near infrared-vacuum dryer fabricated in this study is shown in Figure 1. Drying chamber was a hollow cylinder with inner dimensions of 12·32 cm². In order to thermal insulation, the cylinder is made from Teflon.

A tungsten lamp (100 W) because of its simplicity was used to heat the drying chamber. It was installed at the top of the drying chamber. Distance between end of the lamp and sample tray was about 5 cm. Heating occurs due to filament resistance. Using of various filament diameters enables lamps to be made of similar power but different voltage ratings (Tarrant, 2010). Wavelength spectrum of the tungsten bulb was placed

between 280–6000 nm including waves UV-VIS-IR and more including near infrared wave (Maclasaac et al., 1999).

The air temperatures in the dryer chamber and near the tray sample were recorded using a thermometer with type k sensor and accuracy of ±0.1°C (Lutron TM-903, Taiwan). Air relative humidity was measured by a hygrometer with accuracy of ±3% RH (Lutron TM-903, Taiwan).

The vacuum condition in the drying chamber was created by a vacuum pump (JB-285N, USA). A pressure controller in order to determining and maintaining absolute pressure during the tests with accuracy of 0.001 bar was used (Sensys PSCH0001 BCII, Korea). The sample weight during the experiments was recorded using a digital balance (AND GF-6000, Japan) with ±0.01 g accuracy. Temperature of drying chamber was controlled by a thermostat (Atbin 400k, Iran). A flatbed colour image scanner was used in this experiments (HP Scanjet G4050 Photo Scanner) and setting on 1200 DPI.

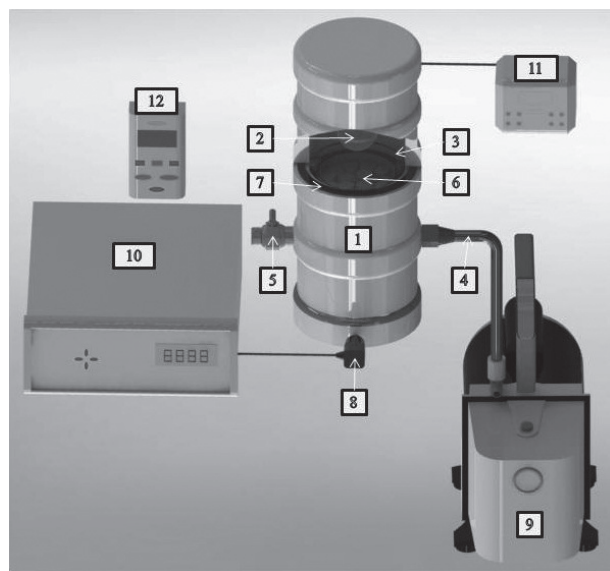


Fig. 1. Scheme of near infrared-vacuum dryer: 1 – drying chamber, 2 – near infrared lamp, 3 – temperature sensor (type k) connected to thermostat, 4 – suction pipe, 5 – vacuum break up valve, 6 – sample tray, 7 – vacuum gasket, 8 – absolute pressure sensor, 9 – vacuum pump, 10 – pressure controller, 11 – thermostat, 12 – thermometer

Modelling of drying kinetics. Moisture ratio during thin layer drying of nectarine slices was calculated as follows:

$$MR = \frac{M - M_e}{M_0 - M_e} \quad (1)$$

where M , M_0 and M_e are the instantaneous moisture content, initial moisture content and equilibrium moisture content, respectively. Equilibrium moisture content (M_e) of samples in each temperature and relative humidity is relatively small compared to M or M_0 (Arumuganathan et al., 2009). Therefore $\frac{(M - M_e)}{(M_0 - M_e)}$ can be simplified as follows:

$$MR = \frac{M}{M_0} \quad (2)$$

Drying curves were fitted with six different moisture ratio models (Table 1). These models are generally achieved by simplifying the general series solutions of Fick's second law and considering a direct relationship between the drying time and average moisture content (Doymaz, 2004). Three different criteria considered for evaluation of best fit: correlation coefficient (R^2), chi square (χ^2) and root mean square error ($RMSE$; Erenturk et al., 2004; Demir et al., 2004).

Table 1. Models employed for fitting of experimental data for thin layer drying of nectarine slices under different absolute pressures

No.	Models name	Equation	References
1	Midilli	$MR = a \cdot \exp(-kt^n) + bt$	Midilli et al. (2002)
2	Page	$MR = \exp(-kt^n)$	Motevali et al. (2011)
3	Wang and Singh	$MR = 1 + at + bt^2$	Wang and Singh (1978)
4	Aghbashlo et al.	$MR = \exp(-at/(1 + bt))$	Aghbashlo et al. (2008)
5	Logarithmic	$MR = a \cdot \exp(-kt) + c$	Wang et al. (2007)
6	Demir et al.	$MR = a \cdot \exp(-kt)^n + b$	Demir et al. (2007)

a, b, c, k and n are drying constants.

$$R^2 = 1 - \frac{\sum_{i=1}^N [MR_{\text{exp},i} - MR_{\text{pre},i}]}{\sum_{k=1}^N \left[MR_{\text{pre},i} - \frac{\sum_{k=1}^n MR_{\text{pre},i}}{N} \right]} \quad (3)$$

$$\chi^2 = \frac{\sum_{i=1}^N (MR_{\text{exp},i} - MR_{\text{pre},i})^2}{N - z} \quad (4)$$

$$RMSE = \left[\frac{1}{N} \sum_{i=1}^N (MR_{\text{exp},i} - MR_{\text{pre},i})^2 \right]^{\frac{1}{2}} \quad (5)$$

where $MR_{\text{exp},i}$ is the experimental moisture ratio of i^{th} data, $MR_{\text{pre},i}$ is the predicted moisture ratio of i^{th} data, N is the number of observations and z is the number of drying constants.

Drying rate. The drying rate of nectarine slices during the thin-layer drying experiments were calculated using the following equations:

$$\text{Drying rate} = \frac{M_{t+dt} - M_t}{dt} \quad (6)$$

where M_t and M_{t+dt} are the moisture content at time t and moisture content at $t + dt$ ($\text{kg}_{\text{water}}/\text{kg}_{\text{dry matter}}$), respectively, t is the drying time (min).

Moisture diffusivity and activation energy. Fick's second law of diffusion equation, symbolized as a mass diffusion equation for drying agricultural products in a falling rate period, is shown in the following equation:

$$\frac{\partial M}{\partial t} = D_{\text{eff}} \frac{\partial^2 M}{\partial x^2} \quad (7)$$

Using appropriate initial and boundary conditions, gave the analytical solutions for various geometries and the solution for slab object (Crank, 1975) with constant diffusivity which is given as:

$$MR = \frac{8}{\pi^2} \sum_{n=0}^{\infty} \frac{1}{(2n+1)^2} \exp\left(- (2n+1)\pi^2 \frac{D_{\text{eff}} \cdot t}{4L^2}\right) \quad (8)$$

where D_{eff} is the effective diffusivity (m^2/s), L is the half thickness of samples (m) and n is a positive integer. For long drying times, only the first term ($n = 0$) in the series expansion of the above equation can give a good estimate of the solution, which is expressed in logarithmic forms as follows (Tutuncu and Labuza, 1996):

$$\ln(MR) = \ln\left(\frac{8}{\pi^2}\right) - \left(\frac{\pi^2}{4L^2} D_{\text{eff}} \cdot t\right) \quad (9)$$

The diffusion coefficients are typically determined by plotting experimental drying data in terms of $\ln(MR)$ versus drying time (t), because the plot gives a straight line with slope of k_1 as:

$$k_1 = \frac{\pi^2 D_{\text{eff}}}{4L^2} \quad (10)$$

The activation energy of nectarine slices was determined using an Arrhenius type equation (Akpınar et al., 2003):

$$D_{\text{eff}} = D_0 \exp\left(-\frac{E_a}{RT}\right) \quad (11)$$

For calculating E_a , eq. (11) can be written as follows:

$$\ln(D_{\text{eff}}) = \ln(D_0) - \left(\frac{E_a}{R}\right)\left(\frac{1}{T}\right) \quad (12)$$

where E_a is the activation energy (kJ/mol), R is the universal gas constant (8.3143 kJ/mol·K), T is the absolute air temperature (K), D_0 is the pre-exponential factor of the equation (m²/s). Plotting $\ln(D_{\text{eff}})$ versus $1/T$ yields a straight line with a slope of k_2 . The coefficient k_2 can be calculated as follows:

$$k_2 = \frac{E_a}{R} \quad (13)$$

Colour. The colour measurements can be used in an indirect way to estimate colour change of foods, since it is simpler and faster than chemical analysis (Maskan, 2000). Most commercial colour measurement instruments are not well suited for food engineering research, because they are designed mainly for quality control. This paper presents a simple method that uses a flatbed scanner to measure colour and the graphics software Photoshop to analyse colour. The term ‘measure’ means that the flatbed scanner is used to obtain the colour values of the pixels on the food surface. The term ‘analyse’ means that Photoshop is used to manipulate those colour values to obtain colour distribution, averages, and so on. Similar this method was reported such as colour of pizza (Yam and Papadakis, 2004) and examine food structure (Stanley and Baker, 2002).

In quantitative analysis, $L^*a^*b^*$ values were used because they are device independent and cover a larger gamut than RGB and CMYK. Photoshop can display $L a b$ values (also RGB and CMYK values) in the info palette and histogram window. The values of a and b in the histogram window are not standard colour values. However, they can be converted to $L^*a^*b^*$ values using the formulas (Yam and Papadakis, 2004):

$$L^* = \frac{\text{Lightness}}{255} \cdot 100 \quad (14)$$

$$a^* = \frac{240a}{255} - 120 \quad (15)$$

$$b^* = \frac{240b}{255} - 120 \quad (16)$$

The total colour difference ΔE was then determined using the following equation:

$$\Delta E = \sqrt{(L_0^* - L_t^*)^2 + (a_0^* - a_t^*)^2 + (b_0^* - b_t^*)^2} \quad (17)$$

Forty samples in each test before and after drying were scanned and data transferred to laptop core i5 with USB port. Then calculated colour mean value L , a and b of forty samples by software photoshop (Adobe photoshop CS6).

Shrinkage. Shrinkage, which occurred during drying as a result of water evaporation, shrinkage coefficient was calculated at each instant of the drying according to the following formula (Dissa et al., 2010):

$$S_b = \left(1 - \frac{V(t)}{V_0}\right) \quad (18)$$

where $V(t)$ is the volume at the instant t (m³) and V_0 is the initial volume of the sample (m³). Three basic sizes measured with the use of a digital caliper. Forty replications were performed on samples with the same moisture content (Figiel, 2010).

Volume. For calculated volume ratio needed the calculated volume of sample that calculated before and after drying according to the following formula:

$$V(t) = A(t) \cdot l(t) \quad (19)$$

where $V(t)$ is the volume at the time t , $A(t)$ is the area of the base and $l(t)$ is the height of the cylinder. $A(t)$ calculated with area of the base that obtained by Photoshop software with cutting around of sample and Enumerated the number of image pixels sample and compared number of square unit pixels with area of 1 cm. This method was tested on several coins with different diameter and have a high accuracy. Value of $l(t)$ was obtained by digital caliper.

Energy consumption. Energy consumed in NIR-vacuum dryer was the total of energy consumed by the vacuum pump and NIR lamp used for warming the dryer space. Energy consumption by vacuum pump can be calculated using eq. (20) (Motevali et al., 2011). The vacuum pump in this dryer are 380 W at 220 V coated electric.

$$E_1 = L_1 \cdot t_1 \quad (20)$$

where E_1 is the power consumed by the pump (kWh), L_1 is the nominal pump power (kW) and t_1 is the total time of turning on the pump (h).

Rate of energy expenditure by the NIR lamps is constant at any given time and is obtained using eq. (21) (Motevali et al., 2011). The IR lamp in this dryer was 100 W at 220 V coated electric.

$$E_2 = L_2 \cdot t_2 \quad (21)$$

E_2 represents the power consumption by the NIR lamp (kW), L_2 is nominal lamp power (kW) and t_2 is total operating time of lamp during drying of pomegranate arils (h). Total energy consumption in NIR-vacuum drying was calculated as follows:

$$E_T = L_1 \cdot E_2 \quad (22)$$

RESULTS AND DISCUSSION

Drying kinetic. Drying curves of nectarine slices undergoing near infrared-vacuum drying at various temperatures are shown in Figure 2. As expected, at the same vacuum level the rate of moisture reduction increased with an increase in the drying temperature because of the increased temperature difference between the drying product and the surrounding, as well as to the increased moisture diffusivity. High temperature is due to turning on the NIR lamp at longer time and samples more exposed the near infrared waves. These results are similar to the previous studies, such as: coconut presscake (Jena and Das, 2007), carrot and pumpkin (Arevalo-Pinedo and Murr, 2007) and onion slice (Mitra et al., 2011).

The rate of moisture reduction increased with a decrease in the absolute pressure of the drying chamber since at lower pressure, water saturates and evaporates at lower temperature. Similar results have been reported in drying of carrot (Cui et al., 2004), Indian

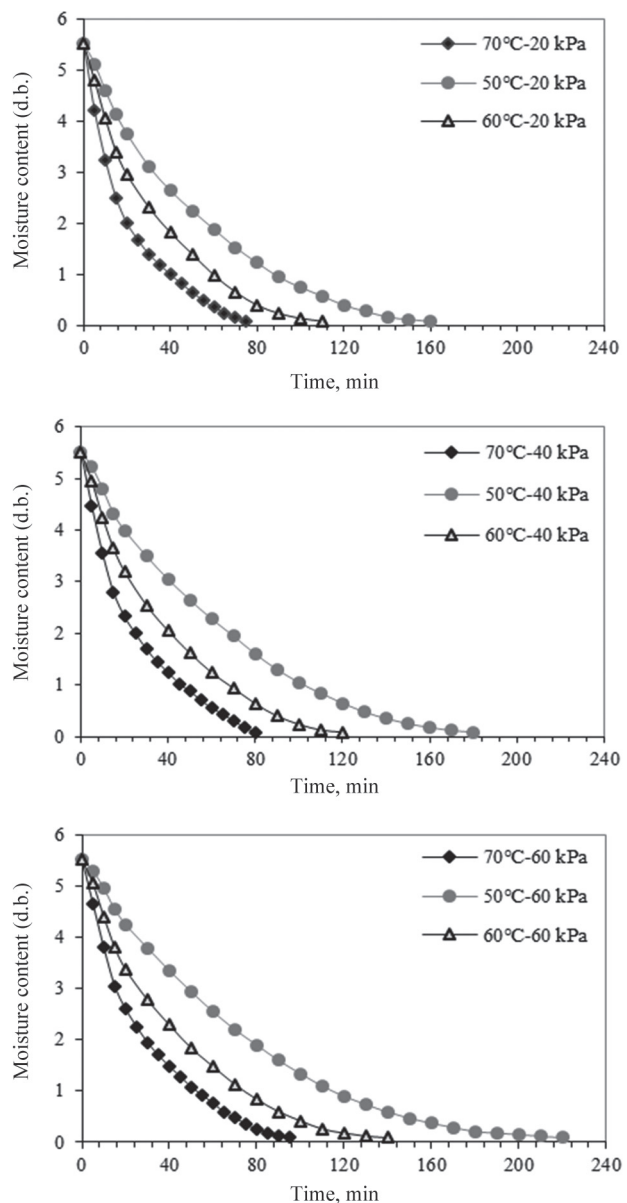


Fig. 2. Effect of drying temperature levels on moisture content of nectarine slices

gooseberry (Methakhup et al., 2005), edamames (Hu et al., 2006), mushroom (Giri and Prasad, 2007) and banana slice (Swasdisevi et al., 2009).

Drying models. The moisture content data from the drying experiments were converted into the moisture

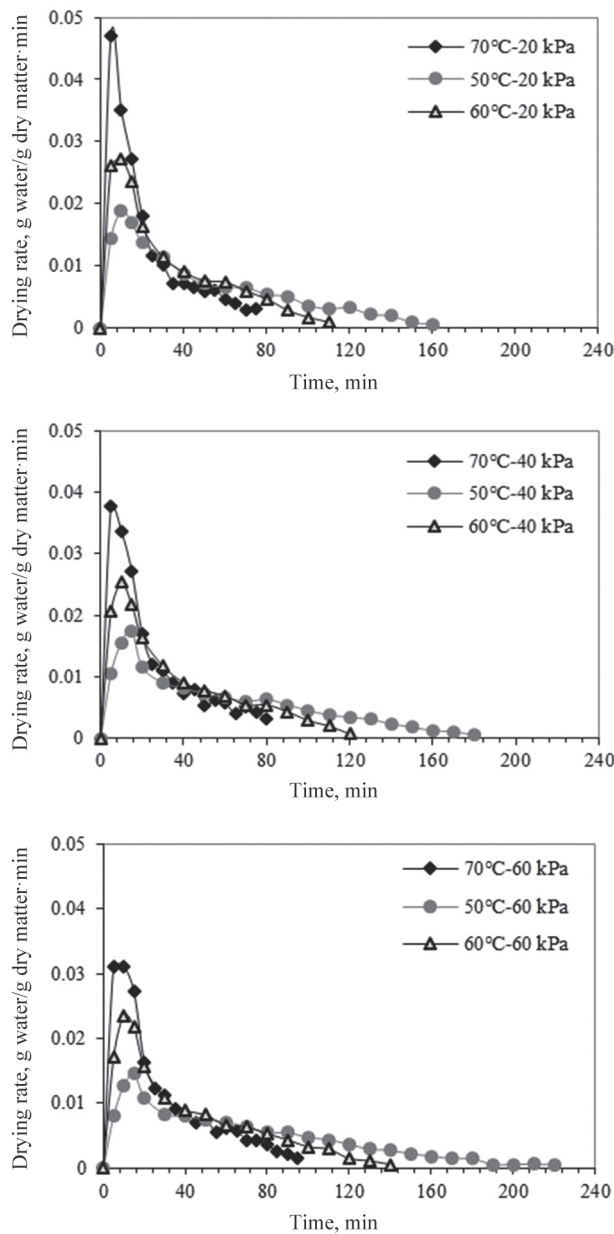


Fig. 3. Variation of drying rate with drying time at various air temperatures and absolute pressures

ratio (*MR*) and then fitted to the selected thin layer drying models listed in Table 1. Six different models were evaluated to find the best model for prediction nectarine slices drying time. Software of MATLAB R2012a with non-linear regression analysis was used

to fit the mathematical models on experimental drying data. The statistical results of the empirical models, including the comparison indices used to evaluate goodness of fit. In the other words, coefficient of determination (R^2), root mean square error (*RMSE*) and reduced chi-square (χ^2) are presented in Figure 3. Based on the criteria of the highest R^2 and the lowest *RMSE* and χ^2 , the best model describing the thin layer drying characteristics of nectarine slices was selected.

For all experiments, the R^2 , *RMSE* and χ^2 values for models changed between 0.9823 and 0.9997, 0.0022 and 0.0821, and 0.0002 and 0.0529, respectively. From Figure 4, the highest R^2 values and the lowest *RMSE* and χ^2 values were obtained from the Midilli model. The R^2 , *RMSE*, and χ^2 values of Midilli model varied between 0.9989 and 0.9997, 0.0022 and 0.0046, and 0.0002 and 0.0005, respectively. Hence the Midilli model was selected as the suitable model to represent the thin layer drying behaviour of nectarine slices Table 2. The estimated values of parameters in Midilli model depends on absolute pressures and drying air temperature. All the estimated parameters were statistically significant at least at 1% level of significance.

The Midilli model has also been suggested by others to describe the infrared drying of tomato (Celma et al., 2008), fluidized bed drying of olive pomace (Arslan and Ozcan, 2011; Meziane, 2011), sun and microwave oven drying of savory leaves and thin layer drying of potato, apple and pumpkin slices (Akpınar, 2006).

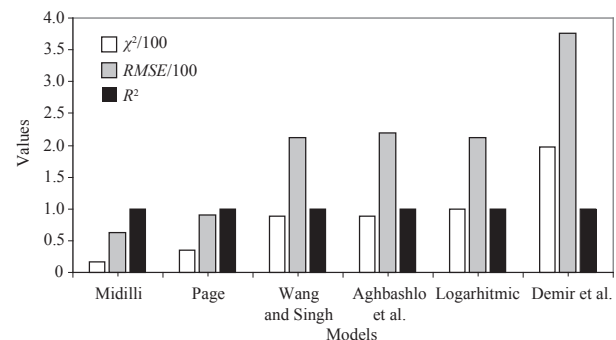


Fig. 4. Average value of R^2 , χ^2 and *RMSE* for used models for fitting of experimental data

Table 2. Estimated values of parameters of midilli model used for thin layer drying of nectarine slices at different absolute pressures

Absolute pressure kPa	Air temperature °C	<i>a</i>	<i>b</i>	<i>k</i>	<i>n</i>	<i>R</i> ²	<i>RMSE</i>	χ^2
20	50	1.017	-0.0001833	0.001585	1.174	0.9994	0.0037	0.0002
	60	1.016	0.0000072	0.002809	1.014	0.9996	0.0024	0.0003
	70	0.9953	-0.00005464	0.000385	1.675	0.9994	0.0046	0.002
40	50	0.9968	0.00000357	0.000275	1.743	0.9997	0.0022	0.0002
	60	1.009	-0.00003189	0.000878	1.236	0.9992	0.0043	0.0004
	70	0.9963	-0.00005664	0.000395	1.678	0.9991	0.0045	0.0003
60	50	0.9948	0.00000357	0.000265	1.874	0.9990	0.0032	0.0002
	60	1.009	-0.00003089	0.000851	1.406	0.9989	0.0033	0.0005
	70	0.9933	-0.00005964	0.000342	1.615	0.9991	0.0035	0.0003

Drying rates. Drying rates of the nectarine slices were calculated using eq. (6). Drying rate changes versus drying time for the absolute pressures and drying air temperature are shown in Figure 3. The drying rates increased with increasing air temperature and decreasing absolute pressures. It is apparent that the drying rate decreased continuously with decreasing moisture content or increasing drying time. Similarly as temperature increased, vapour pressure inside the sample also increased and in turn the pressure gradient between the surface and inner side of the sample increased resulting in a higher drying rate and consequently lesser drying time. This behaviour of decreasing time with increasing drying temperature was also reported for many foodstuffs such as apple pomace (Wang et al., 2007), pumpkin slices (Akpınar, 2006) and onion slices (Jain and Pathare, 2004).

Drying rate showed a fast increase at the beginning of the process sample heating and a subsequent decrease, showing two differentiated periods: the first, where drying rate decreased slowly to reach a plateau with a practically constant value, and the second with a rapidly decreasing drying rate from given critical moisture content. So drying rate curves showed a sigmoid shape where the influence of absolute pressures and drying air temperature can be observed in practically the entire range of sample moisture content.

Similar result has been reported in drying of orange slices (Ruiz Diaz et al., 2003) and mint leaves (Ozbek and Dadali, 2007).

Effective moisture diffusivity. The values of effective moisture diffusivity (D_{eff}) of nectarine slices at different drying conditions obtained by using eq. (10) and the estimated values are presented in Table 3. Also, minimum value belonged to absolute pressure of 60 kPa with air temperature of 50°C and maximum value belonged to absolute pressure of 20 kPa with air temperature of 70°C. These results showed that the higher temperature and lower absolute pressure is better to dry the nectarine slices in the selected experimental domain, because the obtained values of D_{eff} are relatively higher. Also air temperature more than vacuum pressure was factor affecting the D_{eff} of nectarine slices. Furthermore, the values of D_{eff} obtained from this study within the range of $2.46 \cdot 10^{-10}$ to $6.48 \cdot 10^{-10}$ m²/s. These values are comparable for other vacuum dried products such as mango pulp for which the D_{eff} values were reported to be ranging from $1.60 \cdot 10^{-9}$ to $9.20 \cdot 10^{-9}$ m²/s for the temperature range of 65–75°C (Jaya and Das, 2003), Pumpkin freezing the range of $2.01 \cdot 10^{-9}$ to $5.70 \cdot 10^{-9}$ m²/s for the temperature range of 50–70°C (Arevalo-Pinedo and Murr, 2006) and onion slices the range of $1.32 \cdot 10^{-10}$

Table 3. Values of effective diffusivity attained at various air temperatures on near infra-red-vacuum drying of nectarine slices

Air temperature °C	20 kPa		40 kPa		60 kPa	
	D_{eff} m ² /s	R^2	D_{eff} m ² /s	R^2	D_{eff} m ² /s	R^2
50	$3.29 \cdot 10^{-10}$	0.9723	$2.90 \cdot 10^{-10}$	0.9703	$2.46 \cdot 10^{-10}$	0.9859
60	$4.77 \cdot 10^{-10}$	0.9806	$4.34 \cdot 10^{-10}$	0.9721	$3.83 \cdot 10^{-10}$	0.9825
70	$6.48 \cdot 10^{-10}$	0.9705	$5.84 \cdot 10^{-10}$	0.9558	$5.29 \cdot 10^{-10}$	0.9718

to $1.09 \cdot 10^{-9}$ m²/s for the temperature range of 50–70°C (Mitra et al., 2011). When samples were dried at higher temperature, increased heating energy would increase the activity of water molecules leading to higher moisture diffusivity (Xiao et al., 2010).

With multiple regression concurrent relationship values of moisture diffusivity with air temperature and absolute pressure was expressed by following model:

$$D_{\text{eff}} = -3.618 \cdot 10^{-10} + 1.493 \cdot 10^{-11} \cdot T - 2.467 \cdot 10^{-12} \cdot P \quad (23)$$

$$R^2 = 0.9970$$

where T is the air temperature (°C) and P is the absolute pressure (kPa).

Activation energy. Activation energy was calculated from the slope of arrhenius equation by drawing of $\ln(D_{\text{eff}})$ versus $1/(T + 273.15)$ in eq. (13). Figure 5 shows the $\ln(D_{\text{eff}})$ values as a function of absolute temperature. The E_a values of nectarine slices in all absolute pressures are presented in Table 4. E_a of different food and agricultural materials was placed between 12 to 110 kJ/mol (Aghbashlo et al., 2008).

According to the results, E_a of nectarine slices varied between 31.28 and 35.23 kJ/mol for pressures of 20 and 60 kPa, respectively. Similar result has been reported in drying of strawberry (Lee and Hsieh, 2008) and green beans (Doymaz, 2005). Figure 6 shows E_a values of nectarine slices in each absolute pressure. A linear regression model was applied to fit the E_a data set as follows:

$$E_a = 0.0987P + 29.028 \quad (24)$$

$$R^2 = 0.9426$$

R^2 value showed that a good correlation has been established between E_a and absolute pressure. Also

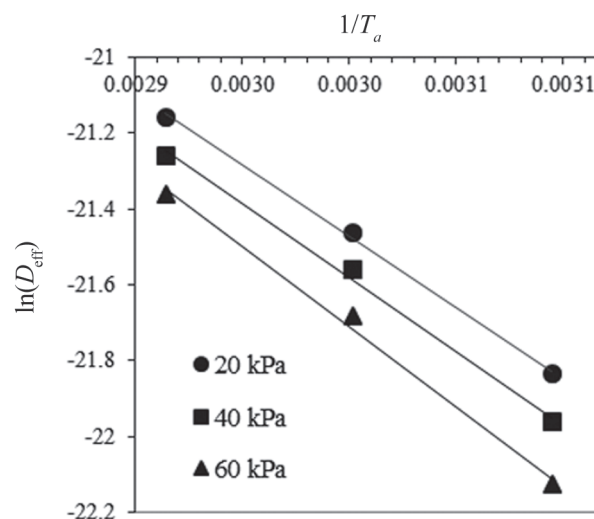


Fig. 5. $\ln(D_{\text{eff}})$ against $1/T_a$ at different absolute pressures for thin-layer drying of nectarine slices

Table 4. Activation energy of nectarine slices in all absolute pressures

	Absolute pressure, kPa		
	20	40	60
E_a , kJ/mol	31.28	32.41	35.23
R^2	0.9985	0.9950	0.9949

with decrease in absolute pressure has caused a decrease in activation energy. This is due to the high level of free water and mass transfer to the nectarine slices surface under vacuum condition.

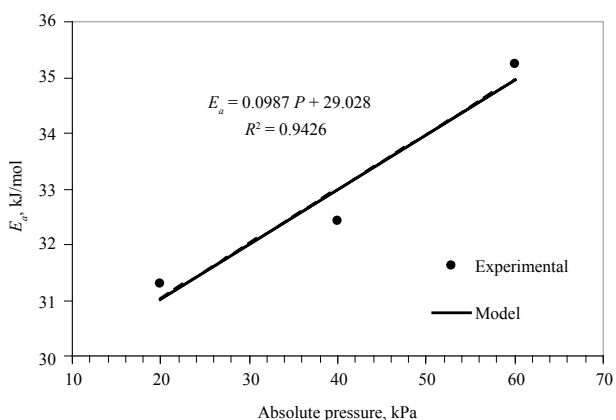


Fig. 6. Influence of absolute pressure on activation energy of nectarine slices

Colour. The plot of ΔE coefficient versus air temperatures and absolute pressures has been presented in Figure 7. Obtained colour value of $L^*a^*b^*$ with L^* representing the brightness or dullness, a^* for redness to greenness, and b^* for yellowness to blueness by the eqs. (14), (15), (16) and finally the total colour difference (ΔE) was then determined using the eq. (17). With increasing air temperature, ΔE was increased and with decreasing vacuum pressure ΔE was decreased (Fig. 7).

When food preparations are heat-processed, a number of chemical reactions occur. One of them is the Millard reaction, known to be responsible for non-enzymatic browning. The Millard reaction involves the reaction of an aldehyde (usually a reducing sugar) and

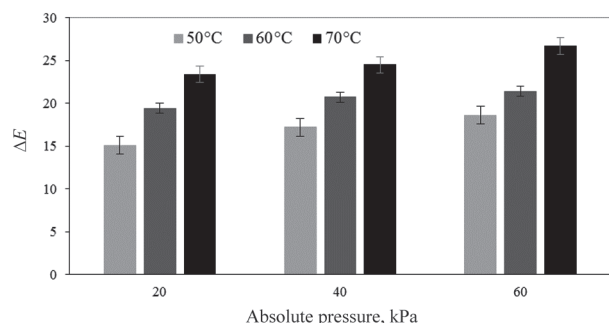


Fig. 7. Plot of total colour difference versus air temperatures and absolute pressures

an amine (usually a protein or amino acid) and is highly temperature dependent. At higher temperature, the degradation pigment processes was increased (Ibarz et al., 1999) with decrease vacuum pressure moisture moving of down layers to surface nectarine slices and continuously coated with a layer of moisture during the initial stage of drying and this layer reduces the effect of heat on surface, resulting in a lower surface reaction such as drying of banana (Chua et al., 2007).

Multiple regression relationship between total colour difference (ΔE) and independent variables air temperature and absolute pressure was proposed as the following model:

$$\Delta E = -5.8560 + 0.3950 \cdot T + 0.0733 \cdot P \quad (25)$$

$$R^2 = 0.9874$$

Shrinkage. The plot of shrinkage coefficient versus air temperatures and absolute pressures has been presented in Figure 8. In each case, forty samples were used and the average values were considered. The shrinkage coefficient of nectarine slices during drying was relatively low compared to that of many foodstuffs with high water content such as fruit and vegetables. The final shrinkage coefficient was from 48.4% to 62.8% whereas for the fruit and vegetables, it was could reach 70% to 90% (Mayor and Sereno, 2004).

When water is removed from a foodstuff, a pressure unbalance is generated between the inner of the material and the external pressure, creates contracting

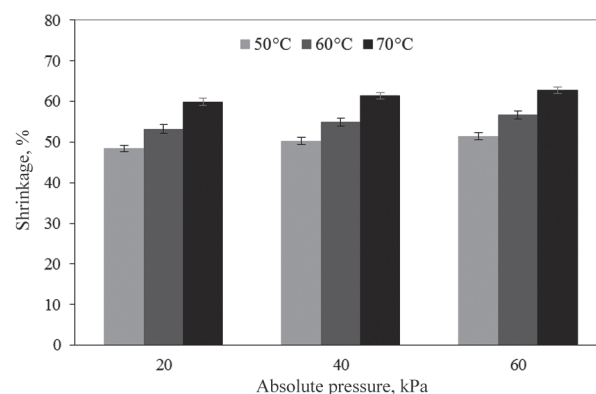


Fig. 8. Plot of shrinkage versus air temperature and absolute pressure

stresses that lead to material shrinkage or collapse, changes in shape and occasionally cracking of the product. This is also the reason why vacuum drying, leads in general to much less shrinkage (Mayor and Sereno, 2004).

Multiple regression relationship between shrinkage coefficient and independent variables (air temperature and absolute pressure) was proposed as the following model:

$$S_b = 18.2 + 0.5683 \cdot T + 0.7833 \cdot P$$

$$R^2 = 0.9938 \quad (26)$$

Energy consumption. Total energy consumption was calculated with eq. (22). The plot of total energy consumption versus air temperatures and absolute pressures has been presented in Figure 9. Total energy consumption of the tests was estimated in the ranges of 0.129 to 0.247 kWh.

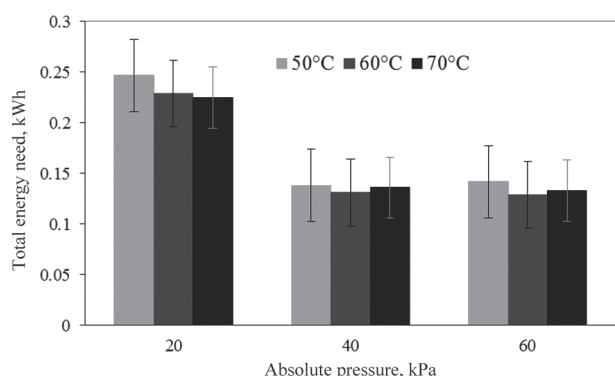


Fig. 9. Plot of total energy consumption versus air temperature and absolute pressure

With decreasing air temperature, total energy consumption increased, because working time of NIR lamp and vacuum pump were increased. Similar result has been reported in drying of pomegranate arils under vacuum conditions (Motevali et al., 2011). Multiple regression relationship between total energy consumption and independent variables (air temperature and absolute pressure) was proposed as the following model:

$$E_T = 7.167 \cdot 10^{-5} \cdot T^2 + 0.0001 \cdot P^2 - 0.0092 \cdot T - 0.0123 \cdot P + 0.7169$$

$$R^2 = 0.9947 \quad (27)$$

CONCLUSIONS

Drying characteristics of nectarine slices were studied in a novel prototype of near infrared-vacuum drying system at the drying temperature range of 50–70°C and the vacuum pressure range of 20–60 kPa. Drying time of nectarine slices decreased with increasing drying temperature and decreasing absolute pressure. The Midilli model provides the best prediction for the thin layer drying characteristics of nectarine slices. This study indicated that based on non-linear regression analysis, the Midilli model gave excellent fitting to the drying experimental data of nectarine slices as a function of the drying temperature or the absolute pressure. Effective moisture diffusivity was increased with decrease of vacuum pressure and increase of drying temperature but effect of drying temperature on effective moisture diffusivity of nectarine slices was more than vacuum pressure. Activation energy was decreased with decrease in absolute pressure. Total colour difference and shrinkage of nectarine slices on near infrared-vacuum drying was decreased with decrease of vacuum pressure and decrease of drying temperature. Energy consumption of the drying nectarine slices was estimated in the ranges of 0.129 to 0.247 kWh.

REFERENCES

- Aghbashlo, M., Kianmehr, M. H., Samimi-Akhijahani, H. (2008). Influence of drying conditions on the effective moisture diffusivity, energy of activation and energy consumption during the thin layer drying of beriberi fruit (*Berberidaceae*). *Ener. Convers. Manag.*, 49(10), 2865–2871.
- Akpinar, E., (2006). Determination of suitable thin layer drying curve model for some vegetables and fruits. *J. Food Eng.*, 73(1), 75–84.
- Akpinar, E., Midilli, A., Bicer, Y. (2003). Single layer drying behaviour of potato slices in a convective cyclone and mathematical modelling. *Ener. Convers. Manag.*, 44(7), 1689–1705.
- AOAC. (2002). Official methods of analysis. Method number 934.06. Association of Official Analytical Chemists Arlington, USA.

- Arevalo-Pinedo, A., Murr, E. X. F. (2006). Kinetics of vacuum drying of pumpkin (*Cucurbita maxima*): Modelling with shrinkage. *J. Food Eng.*, 76(4), 562–567.
- Arevalo-Pinedo, A., Murr, F. E. X. (2007). Influence of pre-treatments on the drying kinetics during vacuum drying of carrot and pumpkin. *J. Food Eng.*, 80(1), 152–156.
- Arslan, D., Ozcan, M. (2011). Evaluation of drying methods with respect to drying kinetics, mineral content, and colour characteristics of savory leaves. *Food Bioproc. Technol.*, 5(3), 983–991.
- Arumuganathan, T., Manikantan, M. R., Rai, R. D., Anandakumar, S., Khare, V. (2009). Mathematical modelling of drying kinetics of milky mushroom in a fluidized bed dryer. *Int. Agrophys.*, 23(1), 1–7.
- Avila, I. M. L. B., Silva, C. L. M. (1999). Modelling kinetics of thermal degradation of colour of peach puree. *J. Food Eng.*, 39(2), 161–166.
- Balch, P. A. (2003). Prescription for dietary wellness. Penguin Group: New York, USA.
- Barreiro, J. A., Milano, M., Sandoval, A. J. (1997). Kinetics of colour change of double concentrated tomato paste during thermal treatment. *J. Food Eng.*, 33(3–4), 359–371.
- Celma, A., Cuadros, F., Rodriguez, L. (2008). Characterisation of industrial tomato by-products from infrared drying process. *Food Bioprod. Process.*, 87(4), 282–291.
- Chua, K. J., Mujumdar, A. S., Chou, S. K., Hawlader, M. N. A., Ho, J. C. (2007). Convective drying of banana, guava and potato pieces: effect of cyclical variations of air temperature on drying kinetics and colour change. *J. Drying Technol.*, 18(4–5), 907–936.
- Crank, J. (1975). The mathematics of diffusion. Clarendon Press: Oxford, UK.
- Cui, Z. W., Xu, S. Y., Sun, D. W. (2004). Microwave-vacuum drying kinetics of carrot slices. *J. Food Eng.*, 65(2), 157–164.
- Dadali, G., Apar, D. K., Ozbek, B. (2007a). Colour change kinetics of okra undergoing microwave drying. *Drying Technol.*, 25(5), 925–936.
- Dadali, G., Demirhan, E., Ozbek, B. (2007b). Colour change kinetics of spinach undergoing microwave drying. *Drying Technol.*, 25(10), 1713–1723.
- Demir, V., Gunhan, T., Yagcioglu, A. K., Degirmencioglu, A. (2004). Mathematical modelling and determination of some quality parameters of air-dried bay leaves. *Biosyst. Eng.*, 88(3), 325–335.
- Demir, V., Gunhan, T., Yagcioglu, A. K. (2007). Mathematical modelling of convection drying of green table olives. *Biosys. Eng.*, 98, 47–53.
- Dissa, A. O., Desmorieux, H., Savadogo, P. W., Segda, B. G., Koulidiati, J. (2010). Shrinkage porosity and density behaviour during convective drying of spirulina. *J. Food Eng.*, 97(3), 410–418.
- Doymaz, I. (2004). Effect of pre-treatments using potassium metabisulphite and alkaline ethyl oleate on the drying kinetics of apricots. *Biosyst. Eng.*, 89(3), 281–287.
- Doymaz, I. (2005). Drying behaviour of green beans. *J. Food Eng.*, 69(2), 161–165.
- Erenturk, S., Gulaboglu, M. S., Gultekin, S. (2004). The thin layer drying characteristics of rosehip. *Biosyst. Eng.*, 89(2), 159–166.
- Figiel, A. (2010). Drying kinetics and quality of beetroots dehydrated by combination of convective and vacuum-microwave methods. *J. Food Eng.*, 98(4), 461–470.
- Ginzburg, A. S. (1969). Application of infrared radiation in food processing. Chem. Proc. Eng. Ser. Leonard Hill: London.
- Giri, S. K., Prasad, S. (2007). Drying kinetics and rehydration characteristics of microwave-vacuum and convective hot-air dried mushrooms. *J. Food Eng.*, 78(2), 512–521.
- Harold, I. Z. (2008). Electromagnetic radiation and toxic exposure. *Human Toxic. Chem. Mix.*, 16, 245–258.
- Hu, Q. G., Min, Z., Mujumdar, A. S., Xiao, G. N., Sun, J. C. (2006). Drying of edamames by hot air and vacuum microwave combination. *J. Food Eng.*, 77(4), 977–982.
- Ibarz, A., Pagan, J., Garza, S. (1999). Kinetic models for colour changes in pear puree during heating at relatively high temperatures. *J. Food Eng.*, 39(4), 415–422.
- Jain, D., Pathare, P. B. (2004). Selection and evaluation of thin layer drying models for infrared radiative and convective drying of onion slices. *Biosyst. Eng.*, 89(3), 289–296.
- Jaya, S., Das, H. (2003). A vacuum drying model for mango pulp. *Drying Technol.*, 21(7), 1215–1234.
- Jena, S., Das, H. (2007). Modelling for vacuum drying characteristics of coconut presscake. *J. Food Eng.*, 79(1), 92–99.
- Krokida, M. K., Maroulis, Z. B., Saravacos, G. D. (2001). The effect of the method of drying on the colour of dehydrated products. *Int. J. Food Sci. Technol.*, 36(1), 53–59.
- Lee, G., Hsieh, F. (2008). Thin-layer drying kinetics of strawberry fruit leather. *Trans. ASABE*, 51, 1699–705.
- Maclasaac, D., Kanner, G., Anderson, G. (1999). Basic physics of the incandescent lamp (Lightbulb). *The Physics Teacher*, 37.
- Maskan, M. (2000). Kinetics of colour change of kiwifruits during hot air and microwave drying. *J. Food Eng.*, 48(2), 169–175.

- Mayor, L., Sereno, A. M. (2004). Modelling shrinkage during convective drying of food materials: a review. *J. Food Eng.*, 61(3), 373–386.
- Meeso, N., Nathakaranakule, A., Midhiyonon, T., Soponronnarit, S. (2004). Influence of FIR irradiation on paddy moisture reduction and milling quality after fluidized bed drying. *J. Food Eng.*, 65(2), 293–301.
- Meeso, N., Nathakaranakule, A., Midhiyonon, T., Soponronnarit, S. (2007). Modelling of far-infrared irradiation in paddy drying process. *J. Food Eng.*, 78(4), 1248–1258.
- Methakhup, S., Chiewchan, N., Devahastin, S. (2005). Effects of drying methods and conditions on drying kinetics and quality of Indian gooseberry flake. *Food Sci. Technol.*, 38(6), 579–587.
- Meziane, S. (2011). Drying kinetics of olive pomace in a fluidized bed dryer. *J. Energy Convers. Manag.*, 52(3), 1644–1649.
- Midilli, A., Kucuk, H., Yapar, Z. (2002). A new model for single-layer drying. *Drying Technol.*, 20(7), 1503–1513.
- Mitra, J., Shrivastava, S. L., Srinivasarao, P. (2011). Vacuum dehydration kinetics of onion slices. *Food Bioprod. Process.*, 89(1), 1–9.
- Motevali, A., Minaei, S., Khoshtaghaza, M. H., Amirnejat, H. (2011). Comparison of energy consumption and specific energy requirements of different methods for drying mushroom slices. *Energy*, 36(11), 6433–6441.
- Nindo, C. I., Kudo, Y., Bekki, E. (1995). Test model for studying sun drying of rough rice using far-infrared radiation. *Drying Technol.*, 13 (1–2), 225–238.
- Nonhebel, G. (1973). *Drying of solids in the chemical industry*. England: Butterworth.
- Ozbek, B., Dadali, G. (2007). Thin-layer drying characteristics and modelling of mint leaves undergoing microwave treatment. *J. Food Eng.*, 83(4), 541–549.
- Pere, C., Rodier, E. (2002). Microwave vacuum drying of porous media: experimental study and qualitative considerations of internal transfers. *Chem. Eng. Process.*, 41(5), 427–436.
- Ratti, C., Mujumdar, A. S. (1995). Infrared drying. In A. S. Mujumdar (Ed.), *Handbook of industrial drying*. Vol. 1 (pp. 567–588). New York: Marcel Dekker.
- Reich, G. (2005). Near-infrared spectroscopy and imaging: basic principles and pharmaceutical applications. *Adv. Drug. Del. Rev.*, 57(8), 1109–1143.
- Ruiz Díaz, G., Martínez-Monzo, P., Chiralt, A. (2003). Modelling of dehydration-rehydration of orange slices in combined microwave/air drying. *Innov. Food Sci. Emerg. Technol.*, 4(2), 203–209.
- Sakai, N., Hanzawa, T. (1994). Applications and advances in far infrared heating in Japan. *Trends Food Sci. Technol.*, 5(11), 357–362.
- Sandu, C. (1986). Infrared radiative drying in food engineering: a process analysis. *Biotechnol. Progress.*, 2(3), 109–119.
- Stanley, D. W., Baker, K. W. (2002). A simple laboratory exercise in food structure/texture relationships using a flatbed scanner. *J. Food Sci. Educ.*, 1, 6–9.
- Strumillo, C., Kudra, T. (1987). *Drying: Principles, applications and design*. USA: Gordon and Breach Sci. Publ.
- Swasdisevi, T., Devahastin, S., Sa-Adchom, P., Soponronnarit, S. (2009). Mathematical modelling of combined far-infrared and vacuum drying banana slice. *J. Food Eng.*, 92(1), 100–106.
- Tarrant, A. W. S. (2010). Optical Measurements. In W. Boyes (Ed.), *Instrumentation reference book* (pp. 499–519). Burlington, USA: Elsevier.
- Tutuncu, M. A., Labuza, T. P. (1996). Effect of geometry on the effective moisture transfer diffusion coefficient. *J. Food Eng.*, 30 (3–4), 433–447.
- Wang, C. Y., Singh, R. P. (1978). A single layer drying equation for rough rice. St. Joseph, MI, USA: ASAE.
- Wang, Z., Sun, J., Liao, X., Chen, F., Zhao, G., Wu, J., Hu, X. (2007). Mathematical modelling on hot air drying of thin layer apple pomace. *J. Food Eng.*, 40(1), 39–46.
- Xiao, H. W., Pang, C. L., Wang, L. H., Bai, J. W., Yang, W. X., Gao, Z. J. (2010). Drying kinetics and quality of Monukka seedless grapes dried in an air-impingement jet dryer. *Biosyst. Eng.*, 105(2), 233–240.
- Yam, K. L., Papadakis, S. E. (2004). A simple digital imaging method for measuring and analyzing colour of food surfaces. *J. Food Eng.*, 61(1), 137–142.

Received – Przyjęto: 21.04.2014

Accepted for print – Zaakceptowano do druku: 16.09.2014

For citation – Do cytowania

Alaei, B., Chayjan, R. A. (2015). Modelling of nectarine drying under near infrared – vacuum conditions. *Acta Sci. Pol. Technol. Aliment.*, 14(1), 15–27. DOI: 10.17306/J.AFS.2015.1.2